

# Quantum Criticality and Global Phase Diagram of Magnetic Heavy Fermions

Qimiao Si

Department of Physics & Astronomy, Rice University, Houston, TX 77005, USA

PACS 71.10.Hf, 71.27.+a, 75.20.Hr, 71.28.+d

Corresponding author: e-mail qmsi@rice.edu

Quantum criticality describes the collective fluctuations of matter undergoing a second-order phase transition at zero temperature. It is being discussed in a number of strongly correlated electron systems. A prototype case occurs in the heavy fermion metals, in which antiferromagnetic quantum critical points have been explicitly observed. Here, I address two types of antiferromagnetic quantum critical points. In addition to the standard description based on the fluctuations of the antiferromagnetic order, a local quantum critical point is also considered.

It contains inherently quantum modes that are associated with a critical breakdown of the Kondo effect. Across such a quantum critical point, there is a sudden collapse of a large Fermi surface to a small one. I also consider the proximate antiferromagnetic and paramagnetic phases, and these considerations lead to a global phase diagram. Finally, I discuss the pertinent experiments on the antiferromagnetic heavy fermions, briefly address the case of ferromagnetic heavy fermions, and outline some directions for future studies.

Copyright line will be provided by the publisher

**1 Introduction** A quantum critical point (QCP) refers to a second-order phase transition at zero temperature. The notion of quantum criticality is playing a central role in a number of strongly correlated systems, but this was not anticipated when it was first introduced. Indeed, the initial work of Hertz [1] was rather modest. From the critical phenomenon perspective, Hertz formulated a direct extension of Wilson's then-newly-completed renormalization-group (RG) theory of classical critical phenomena [2]. The formulation retained the basic property of the latter: the zero-temperature phases are still considered to be distinguished by an order parameter, a coarse-grained macroscopic variable characterizing the breaking of a global symmetry of the Hamiltonian, and the critical modes are the fluctuations of the order parameter. In this sense, it retains the Landau paradigm for phase transitions. From a microscopic perspective, Hertz's discussion built on the historical work about paramagnons, the overdamped magnons occurring in a paramagnetic metal as it becomes more and more ferromagnetic (for a review, see Ref. [3]). In hindsight, the convergence of these two lines of theoretical physics seems to be rather natural. For a Stoner ferromagnet, the fluctua-

tions of the order parameter (magnetization) at its QCP is none other but the paramagnons. For a spin-density-wave (SDW) antiferromagnet, such fluctuations of the order parameter (staggered magnetization) are correspondingly antiparamagnons. For completeness, it is interesting to note on the third line of activities predating Hertz's work. A QCP was already contained in the microscopic solution of an Ising chain in a transverse field [4], and this solution was being reformulated in the Landau framework [5].

The order-parameter fluctuations of a classical magnetic critical point is specified by a  $d+1$  field theory in  $d$ -spatial dimensions [2]. Within the Hertz formulation, quantum mechanics introduces mixing between the statics and dynamics, and the corresponding critical point is described by the  $d+1$  theory in  $d+1$  dimensions. Here,  $z$  is the dynamic exponent;  $z = 3$  for the QCP of the Stoner ferromagnet,  $z = 2$  for the SDW QCP, and  $z = 1$  for the transverse-field Ising model. Within this framework, an important observation, first discussed for a QCP of an insulating magnet in two dimensions [6, 7], is that a QCP at  $T = 0$  will influence physical properties at finite temperatures over a finite-range of non-thermal control parameters.

Copyright line will be provided by the publisher

While quantum criticality is currently being discussed in a number of strongly correlated systems [8], it has arguably been most systematically studied in magnetic heavy fermion metals [9,10,11]. From a materials perspective, the heavy fermions have a number of advantages in this context. In particular, the large effective electronic mass – the defining characteristics of these systems – implies that the relevant energy scales are small, making it relatively easy to tune their ground states by external parameters such as magnetic field or pressure [12]. At the same time, the understanding of their effective Hamiltonian – containing competing Kondo and RKKY interactions [13, 14, 15] – gives us intuition on how the system is being tuned microscopically when an external non-thermal control parameter is varied. Explicit observation of AF QCPs has been made in a number of heavy fermion metals [9,10], including, in particular,  $\text{CeCu}_6-x\text{Au}_x$ ,  $\text{YbRh}_2\text{Si}_2$ , and  $\text{CePd}_2\text{Si}_2$ . These systems have allowed systematic probes of quantum critical behavior through transport, thermodynamic, and spectroscopic measurements. One very basic lesson is that the influence of quantum critical fluctuations can cover a large control-parameter range at non-zero temperatures, and can extend to surprisingly high temperatures [9, 10, 11].

Theoretically, an important notion that has emerged is that QCPs can go beyond the Landau paradigm. The new type of QCPs being discussed contains critical excitations that are inherently quantum-mechanical, in the form of a critical breakup of Kondo singlets [16,17,18,19]. The notion that there could be emergent quantum excitations beyond order-parameter fluctuations is, while un-orthodox, in fact natural. After all, the order parameters we are dealing with are coarse-grained classical variables. It is conceivable that genuine quantum-mechanical effects – associated with the Kondo entanglement effect in our case – are part of the critical fluctuations at a QCP. These considerations have enjoyed fruitful interactions with experimental studies in the heavy fermion systems on spin dynamics [20,21,22,23], Fermi surface [24,25,26], and multiple energy scales [24,25,27]. More broadly, they have impacted on the developments of QCPs in other systems as well, including in insulating quantum magnets [28]. It appears that the many-body-theory community has largely come to terms with the notion that QCPs exist beyond the Landau paradigm.

**2 Kondo lattice and heavy Fermi liquid** Heavy fermions were traditionally considered as a prototype for a strongly correlated Fermi liquid. The theory of a heavy Fermi liquid was developed in the early 1980s [13]. The microscopic model for the magnetic heavy fermion materials is the Kondo lattice Hamiltonian:

$$H = \frac{1}{2} \sum_{i,j} I_{ij} S_i \cdot S_j + \sum_k \epsilon_k \sum_{\sigma} c_{k\sigma}^\dagger c_{k\sigma} + \sum_i J_K S_i \cdot \mathbf{S}_i \quad (1)$$

The model contains a lattice of spin-1=2 local moments, which interact with each other with an AF exchange interaction  $I_{ij}$ ; we will use  $I$  to label say the nearest-neighbor interaction. It also includes a conduction-electron band,  $\epsilon_k$ , with a band dispersion  $\epsilon_k$  (and, correspondingly, a hopping matrix  $t_{ij}$ );  $W$  labels the bandwidth. At each site  $i$ , the spin of the conduction electrons,  $\mathbf{S}_{i,c} = (1=2) \sum_{\alpha} c_{i\alpha}^\dagger \boldsymbol{\sigma}_{\alpha} c_{i\alpha}$ , where  $\boldsymbol{\sigma}_{\alpha}$  are the Pauli matrices, is coupled to a spin-1=2 local moment,  $\mathbf{S}_i$ , via an AF Kondo exchange interaction  $J_K$ .

The Kondo screening effect leads to Kondo resonances, which are charge-e and spin-1=2 excitations. There is one such Kondo resonance per site, and these excitations induce a “large” Fermi surface. Consider that the conduction electron band is filled with  $x$  electrons per site; for concreteness, we take  $0 < x < 1$ . The conduction electron band and the Kondo resonances will be hybridized, resulting in a count of  $1 + x$  electron per site. The Fermi surface would therefore have to expand to a size that encloses all these  $1 + x$  electrons. This defines the large Fermi surface [13,29,30,31].

In the regime  $I \ll J_K \ll W$ , various approaches, in particular the slave-boson mean field theory [13,29,30], give rise to the following picture. Consider the conduction electron Green’s function:

$$G_c(\mathbf{k}; \omega) = \langle \langle c_{\mathbf{k}}(\omega) c_{\mathbf{k}}^\dagger(0) \rangle \rangle \quad (2)$$

where  $\langle \langle \dots \rangle \rangle$  is taken with respect to  $\omega$ . This Green’s function is related to a self-energy,  $\Sigma(\mathbf{k}; \omega)$ , via the standard Dyson equation:

$$G_c(\mathbf{k}; \omega) = \frac{1}{\omega - \epsilon_{\mathbf{k}} - \Sigma(\mathbf{k}; \omega)} \quad (3)$$

In the heavy Fermi liquid state,  $\Sigma(\mathbf{k}; \omega)$  is non-analytic and contains a pole in the energy space:

$$\Sigma(\mathbf{k}; \omega) = \frac{(\omega - \epsilon_{\mathbf{k}})^2}{\omega - \epsilon_{\mathbf{k}} - \epsilon_f} \quad (4)$$

Inserting Eq. (4) into Eq. (3), we end up with two poles in the Green’s function:

$$G_c(\mathbf{k}; \omega) = \frac{u_{\mathbf{k}}^2}{\omega - \epsilon_{1;\mathbf{k}}} + \frac{v_{\mathbf{k}}^2}{\omega - \epsilon_{2;\mathbf{k}}} \quad (5)$$

Here,

$$\epsilon_{1;\mathbf{k}} = (1=2) \epsilon_{\mathbf{k}} + \epsilon_f \frac{h}{\hbar} \frac{q}{(k - \epsilon_f)^2 + 4(\omega)^2}; \quad \epsilon_{2;\mathbf{k}} = (1=2) \epsilon_{\mathbf{k}} + \epsilon_f + \frac{h}{\hbar} \frac{q}{(k - \epsilon_f)^2 + 4(\omega)^2} \quad (6)$$

describe the dispersion of the two heavy-fermion bands. These bands must accommodate  $1 + x$  electrons, so the new Fermi energy has to lie in a relatively flat portion of the dispersion, leading to a small Fermi velocity and a large quasiparticle mass  $m^*$ .

It is important to make a note here that we have used a  $k$ -independent self-energy to induce a large reconstruction of the quasiparticle dispersion ( $\epsilon_{\mathbf{k}} \rightarrow \epsilon_{1;\mathbf{k}}; \epsilon_{2;\mathbf{k}}$ ) and

a corresponding large reconstruction of the Fermi surface. In fact, the self-energy of Eq. (4) contains only two parameters, the pole strength (*i.e.*, the residue),  $(b)^2$ , and the pole location,  $\epsilon_f$ . Eq. (4) does not contain the incoherent features beyond the well-defined pole. Such incoherent components can be introduced, through  $\epsilon_{\text{SDW}}$ : the dynamical mean field theory [32,33,34,35], and they will induce non-zero damping (of the Fermi liquid form) to the quasi-particle excitations in Eq. (5). But the fact remains that a  $k$ -independent self-energy is adequate to capture the Kondo effect and the resulting heavy quasiparticles. We will return to this feature shortly in the discussion of a Kondo breakdown effect.

### 3 Quantum criticality in the Kondo lattice

**3.1 General considerations** The Kondo interaction drives the formation of Kondo singlets between the local moments and conduction electrons. At high temperatures, the system is in a fully incoherent regime with the local moments weakly coupled to conduction electrons. Going below some scale  $T_K^0$ , the initial screening of the local moments starts to set in. Eventually, at temperatures below some Fermi-liquid scale,  $T_{FL}$ , the heavy quasiparticles are fully developed.

When the AF RKKY interaction among the local moments becomes larger than the Kondo interaction, the system is expected to develop an AF order. An AF QCP is then to be expected, when the control parameter,  $\mu = T_K^0$ , reaches some critical value  $\mu_c$ . At  $\mu > \mu_c$ , the AF order will develop as the control parameter is lowered through the AF-ordering line,  $T_N(\mu)$ .

In addition, the RKKY interactions will also eventually lead to the suppression of the Kondo singlets. Qualitatively, the RKKY interactions promote singlet formation among the local moments, thereby reducing the tendency of singlet formation between the local moments and conduction electrons. This will define an energy ( $E_{loc}$ ) or temperature ( $T_{loc}$ ) scale, describing the breakdown of the Kondo effect. On very general grounds, the  $T_{loc}$  line is expected to be a crossover at non-zero temperatures, but a sharp transition at zero temperature.

To study these issues theoretically, one key question is how to capture not only the magnetic order and Kondo-screening, but also the dynamical competition between the Kondo and RKKY interactions. The microscopic approach that is capable of doing this is the extended dynamical mean field theory (EDMFT) [36,37,38]. The two solutions [16,39,40,41,42,43,44,45] that have been derived through EDMFT are summarized below.

Large-N approaches based on slave-particle representations of the spin operator are also commonly used to study Kondo-like systems. One type of approach is based on a fermionic representation of the spin [18,19]. This representation naturally incorporates the physics of singlet formation, so it captures the Kondo singlets (as well as the singlets among the local moments), but it does not

allow magnetism in the large-N limit. One may allow a magnetic order in a static mean-field theory for a finite-N [18]. However, the magnetic transition and breakdown of Kondo screening are always separated in the phase diagram and the zero-temperature magnetic transition is still of the SDW type. This, we believe, is a manifestation of the static nature of the mean field theory.

A Schwinger-boson-based large-N formulation is another microscopic approach that is being considered in this context [46]. This approach naturally incorporates magnetism. While it is traditionally believed that bosonic representations of spin in general have difficulty to capture the Kondo screening physics at its large-N limit, there is indication [46] that the dynamical nature of the formulation here allows an access to at least aspects of the Kondo effect. It will be interesting to see what type of quantum phase transitions this approach will lead to for the Kondo lattice problem.

This is a subject that is still in a very rapid development, and a number of other theoretical approaches are also being taken [47,48,49,50].

**3.2 Microscopic approach based on the extended dynamical mean field theory** The EDMFT method incorporates intersite collective fluctuations into the dynamical mean field theory framework [32,33]. This systematic method is constructed within a “cavity”, diagrammatic, or functional formalism [36,37,38]. It is conserving, satisfying the various Ward identities. Diagrammatically, EDMFT incorporates an infinite series associated with intersite interactions, in addition to the local processes already taken into account in the dynamical mean field theory.

Within the EDMFT, the dynamical spin susceptibility and the conduction-electron Green’s function respectively have the forms:  $\chi(q; \omega) = \frac{1}{M(q; \omega) + i\eta}$ , and  $G(k; \omega) = \frac{1}{\epsilon_k - \omega + i\eta}$ . The correlation functions,  $\chi(q; \omega)$  and  $G(k; \omega)$ , are momentum-dependent. At the same time, the irreducible quantities,  $M(q; \omega)$  and  $\epsilon_k$  are momentum-independent. They are determined in terms of a Bose-Fermi Kondo model,

$$H_{\text{imp}} = \sum_{\mathbf{p}} J_{\mathbf{K}} S_{\mathbf{p}} \sum_{\mathbf{p}'} \sum_{\mathbf{p}''} E_{\mathbf{p}} C_{\mathbf{p}}^{\dagger} C_{\mathbf{p}'} + \sum_{\mathbf{p}} g_{\mathbf{p}} S_{\mathbf{p}} + \sum_{\mathbf{p}} \sum_{\mathbf{p}'} w_{\mathbf{p}} C_{\mathbf{p}}^{\dagger} C_{\mathbf{p}'} + \sum_{\mathbf{p}} \sum_{\mathbf{p}'} w_{\mathbf{p}}^{\dagger} C_{\mathbf{p}} C_{\mathbf{p}'}^{\dagger} \quad (7)$$

The fermionic and bosonic baths are determined by self-consistency conditions, which manifest the translational invariance,  $\chi_{loc}(q; \omega) = \chi(q; \omega)$ , and  $G_{loc}(k; \omega) = G(k; \omega)$ .

The 0 + 1-dimensional quantum impurity problem, Eq. (7), has the following Dyson equations:  $M(q; \omega) = \chi_0^{-1}(q; \omega) + 1 = \chi_{loc}^{-1}(q; \omega)$  and  $\epsilon_k = G_0^{-1}(k; \omega) - 1 = G_{loc}^{-1}(k; \omega)$ , where  $\chi_0^{-1}(q; \omega) = \sum_{\mathbf{p}} \sum_{\mathbf{p}'} \frac{J_{\mathbf{K}}^2}{2w_{\mathbf{p}}} [1 - \frac{w_{\mathbf{p}}^2}{w_{\mathbf{p}'}}]$  and  $G_0^{-1}(k; \omega) =$

$\Gamma_{\mathbf{q}}^{-1} = \sum_{\mathbf{p}} \chi(\mathbf{p}) \chi(\mathbf{p} + \mathbf{q})$  are the Weiss fields. The EDMFT formulation allows us to study different degrees of quantum fluctuations as manifested in the spatial dimensionality of these fluctuations. The case of two-dimensional magnetic fluctuations are represented in terms of the RKKY density of states that has a non-zero value at the lower edge, eg.:

$$\chi(\mathbf{q}) = \frac{1}{\Omega} \sum_{\mathbf{p}} \chi(\mathbf{p}) \chi(\mathbf{p} + \mathbf{q}) = \frac{1}{2\Omega} \sum_{\mathbf{p}} \chi(\mathbf{p}) \chi(\mathbf{p} - \mathbf{q}) + \frac{1}{2\Omega} \sum_{\mathbf{p}} \chi(\mathbf{p}) \chi(\mathbf{p} + \mathbf{q}) \quad (8)$$

where  $\Theta(x)$  is the Heaviside step function. Likewise, three-dimensional magnetic fluctuations are described in terms of  $\chi(\mathbf{q})$  which vanishes at the lower edge in a square-root fashion, for example:

$$\chi(\mathbf{q}) = \frac{1}{\Omega} \sum_{\mathbf{p}} \chi(\mathbf{p}) \chi(\mathbf{p} + \mathbf{q}) = \frac{1}{2\Omega} \sum_{\mathbf{p}} \chi(\mathbf{p}) \chi(\mathbf{p} - \mathbf{q}) + \frac{1}{2\Omega} \sum_{\mathbf{p}} \chi(\mathbf{p}) \chi(\mathbf{p} + \mathbf{q}) \quad (9)$$

The bosonic bath reflects the effect of the dynamical magnetic correlations, primarily among the local moments, on the local Kondo effect. On approach to a magnetic quantum critical point, its spectrum turns soft, and its ability to suppress the Kondo effect increases. This effect has been explicitly seen in a number of specific studies [16,39,40,41,42,43,44,45]. Moreover, the zero-temperature transition is second-order whenever the same form of the effective RKKY interaction appears in the formalism on both sides of the transition [51,52].

**3.3 Spin-density-wave QCP** The reduction of the Kondo-singlet amplitude by the dynamical effects of the RKKY interactions among the local moments has been considered in some detail in a number of studies based on EDMFT [16,39,40,41,42,43,44,45]. Irrespective of the spatial dimensionality, this weakening of the Kondo effect is seen through the reduction of an  $E_{\text{loc}}$  scale.

Two classes of solutions emerge depending on whether this Kondo breakdown scale vanishes at the AF QCP. In the case of Eq. (9),  $E_{\text{loc}}$  has not yet been completely suppressed to zero when the AF QCP,  $Q_c$ , is reached from the paramagnetic side (but it can go to zero inside the AF region, as further discussed in Sec. 4). The quantum critical behavior, at energies below  $E_{\text{loc}}$ , falls within the Hertz-Moriya-Millis type [1,53,54]. The zero-temperature dynamical spin susceptibility has the following form:

$$\chi(\mathbf{q}; i\omega) = \frac{1}{f(\mathbf{q}) - i\omega} \quad (10)$$

Here  $f(\mathbf{q}) = \chi_{\mathbf{q}}^{-1}$ , and is generically  $\propto |\mathbf{q} - \mathbf{Q}|^2$  as the wavevector  $\mathbf{q}$  approaches the AF ordering wavevector  $\mathbf{Q}$ . The QCP is described by a Gaussian fixed point. At non-zero temperatures, a dangerously irrelevant operator invalidates the so-called  $\omega = T$  scaling [54].

**3.4 Local quantum critical point** Another class of solution corresponds to  $E_{\text{loc}} = 0$  already at  $Q_c$ . It arises in the case of Eq. (8), where the quantum critical magnetic fluctuations are strong enough to suppress the Kondo effect.

The solution to the local spin susceptibility has the form:

$$\chi(\mathbf{q}; i\omega) = \frac{1}{f(\mathbf{q}) + A(\mathbf{q}; i\omega)W(\omega = T)} \quad (11)$$

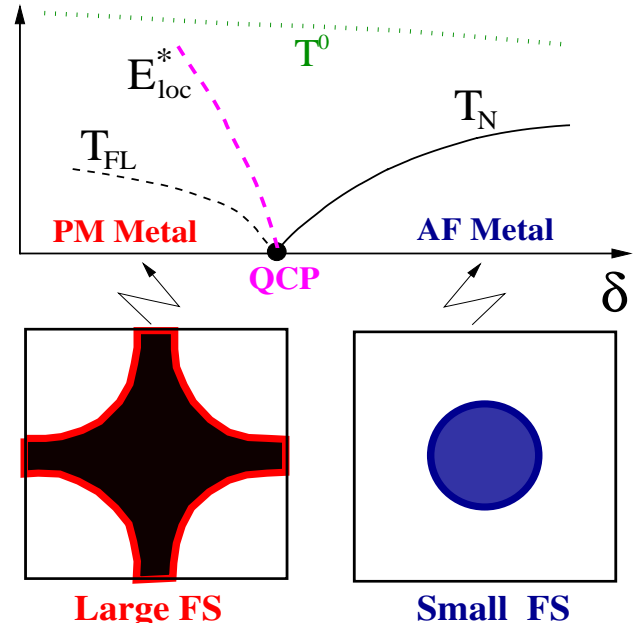


**Figure 1** Illustration of the local quantum critical point, which has a critical breakdown of the Kondo effect. The  $E_{\text{loc}}$  scale separates between the regimes where the system goes towards either the Kondo-screened paramagnetic metal ground state or the Kondo-destroyed AF metal ground state. The Fermi surface goes from being large in the paramagnetic metal phase to being small in the AF metal phase.  $T^0$  is the scale at which the initial Kondo screening sets in as temperature is lowered from above  $T^0$ .

This expression was derived [16,39] within the EDMFT studies, and through the aid of an  $\omega$ -expansion approach to the Bose-Fermi Kondo model. At the AF QCP, the Kondo effect itself is critically destroyed (*cf.* Fig. 1). The calculation of the critical exponent  $\nu$  is beyond the reach of the  $\omega$ -expansion. In the Ising-anisotropic case,  $\nu$  has been calculated numerically [40,43,44,45]: it is fractional, and is about 0.7.

The breakdown of the Kondo effect not only affects magnetic dynamics, but also influences the single-electron excitations. As the QCP is approached from the paramagnetic side, the quasiparticle residue  $z_L \propto \nu$ , the strength of the pole of  $\chi(\mathbf{q}; i\omega)$  [*cf.* Eq. (4)], goes to zero. The large Fermi surface turns critical.

The breakdown of the large Fermi surface suggests that the Fermi surface will be small on the antiferromagnetically ordered side. This leads us to the issue of the Kondo effect inside the AF phase, which we now discuss in some detail.

**4 Antiferromagnetism and Fermi surface in Kondo lattices** To consider the Kondo effect in the ordered phase, we focus on the parameter regime of the Kondo lattice model, Eq. (1), in the the limit  $J_K \gg \Gamma$

$W$ . Here  $I$  is the scale for the RKKY exchange interaction, and  $W$  the bandwidth of the conduction-electron band.

In this limit, we can use as our reference point the  $J_K = 0$  case [55]. At this reference point, the local moments with AF exchange interactions are decoupled from the conduction electrons. We will focus on the case that the local-moment system itself is in a collinear AF state. The low-energy theory for the local-moment Hamiltonian [the first term of Eq. (1)] is the quantum non-linear sigma model (QNL  $\sigma$ ) [56, 6]:

$$S_{\text{QNL } \sigma} = \frac{c}{2g} \int d^d x d\tau \left[ (\partial_\mu \mathbf{n})^2 + \frac{g}{c} \mathbf{n} \cdot \partial_\mu \mathbf{n} \right] \quad (12)$$

Here  $c$  is the spin-wave velocity, and  $g$  describes the quantum fluctuations. There are gapless excitations in two regions of the wavevector space: the staggered magnetization ( $\mathbf{q}$  near  $\mathbf{Q}$ ) specified by the  $\mathbf{n}$  field and the uniform magnetization ( $\mathbf{q}$  near 0) described by  $\mathbf{n} = \langle \mathbf{n} \rangle + \delta \mathbf{n}$ .

When the Fermi surface of the conduction electrons does not intersect the AF zone boundary, only the uniform component of the local moments can be coupled to the spins of the conduction-electron states near the Fermi surface. The effective Kondo coupling takes the form,

$$S_K = \int d^d x d\tau \sum_{\mathbf{n}} \delta \mathbf{n} \cdot \mathbf{s} \quad (13)$$

A momentum-shell RG treatment requires a procedure that mixes bosons, which scale along all directions in momentum space [2], and fermions, which scale along the radial direction perpendicular to the Fermi surface [57]. Using the procedure specified in Ref. [58], we found  $\delta \mathbf{n}$  to be marginal at the leading order [55], just like in the paramagnetic case. The difference from the latter appears at the loop level:  $\delta \mathbf{n}$  is exactly marginal to infinite loops [55].

The fact that  $\delta \mathbf{n}$  does not run towards infinity implies a breakdown of the Kondo effect. This is supplemented by a large  $N$  calculation [55], which showed that the effective Kondo coupling, Eq. (13), leads to the following self-energy for the conduction electrons:

$$\langle \mathbf{k}; \tau \rangle / \tau^d : \quad (14)$$

The absence of a pole in  $\langle \mathbf{k}; \tau \rangle$ , in contrast to Eq. (4), implies the absence of any Kondo resonance. Correspondingly, the Fermi surface is small.

When the Fermi surface of the conduction electrons intersects the AF zone boundary [59], the staggered magnetization,  $\mathbf{n}$ , can be directly coupled to the spins of the conduction electrons. However, this coupling is proportional to  $\mathbf{q} \cdot \mathbf{Q}$ , as dictated by Adler's theorem. The Kondo coupling remains marginal, and the Fermi surface remains small.

## 5 Towards a global phase diagram

**5.1 How to melt a Kondo-destroyed antiferromagnet** Given the understanding that the AF state with a small Fermi surface is a stable phase, it would be illuminating to approach the quantum transition from this ordered state.

One may consider to use the QNL  $\sigma$  representation, and study the transition by increasing the effective Kondo coupling,  $J_K$  of Eq. (13). A recent study, using an RG analysis of an action closely related to that discussed in Sec. 4 but with the conduction electrons integrated out, has gone along this direction [60]. Such an analysis, however, cannot capture the overall phase diagram of the Kondo lattice systems. What is missing so far is the Berry-phase term of the QNL  $\sigma$  representation:

$$S_{\text{Berry}} = i s \int d^d x d\tau \sum_{\mathbf{x}} \mathbf{A}_{\mathbf{x}} \cdot \dot{\mathbf{n}} \quad (15)$$

Here,  $s = \frac{1}{2}$  is the size of the local-moment spin,  $A_{\mathbf{x}}$  is the area on the unit sphere spanned by  $\mathbf{n}(\mathbf{x}; \tau)$  with  $\tau \in [0; \tau_0]$ , and  $\mathbf{x} = \mathbf{0}$  at even/odd sites (consider, for definiteness, a cubic or square lattice with Néel order).

The Berry phase term can be neglected deep inside the AF phase. For smooth configurations of  $\mathbf{n}$  in the  $(\mathbf{x}; \tau)$  space, the Berry phase term vanishes. Topologically non-trivial configurations of  $\mathbf{n}$  in  $(\mathbf{x}; \tau)$  yield a finite Berry phase. They, however, cost a non-zero energy inside the AF phase and can be neglected for small  $J_K$  and, correspondingly, small  $\tau_0$ . As  $J_K$  is increased, on the other hand, these gapped configurations come into play. Indeed, they are expected to be crucial for capturing the Kondo effect. Certainly, the Kondo singlet formation requires the knowledge of the size of the microscopic spins, and the Berry phase term is what encodes the size of the spin in the QNL  $\sigma$  representation.

**5.2 Global phase diagram** We can address these effects at a qualitative level, in terms of a global phase diagram. We consider a two-dimensional parameter space [61], as shown in Fig. 2. The vertical axis describes the local-moment magnetism. It is parametrized by  $G$ , which characterizes the degree of quantum fluctuations of the local-moment magnetism; increasing  $G$  reduces the Néel order. This parameter can be a measure of magnetic frustration, e.g.  $G = J_{n,n+1}/J_{n,n}$ , the ratio of the next-nearest-neighbor exchange interaction to the nearest-neighbor one, or it can be the degree of spatial anisotropy. The horizontal axis is  $\tilde{J}_K = J_K/W$ , the Kondo coupling normalized by the conduction-electron bandwidth. We are considering a fixed value of  $I=W$ , which is typically much less than 1, and a fixed number of conduction electrons per site, which is taken to be  $0 < x < 1$  without a loss of generality.

The  $AF_S$  phase describes the small-Fermi-surface AF state, whose existence has been established asymptotically exactly using the RG method as described in the previous section. The  $PL$  phase is the standard heavy Fermi liquid

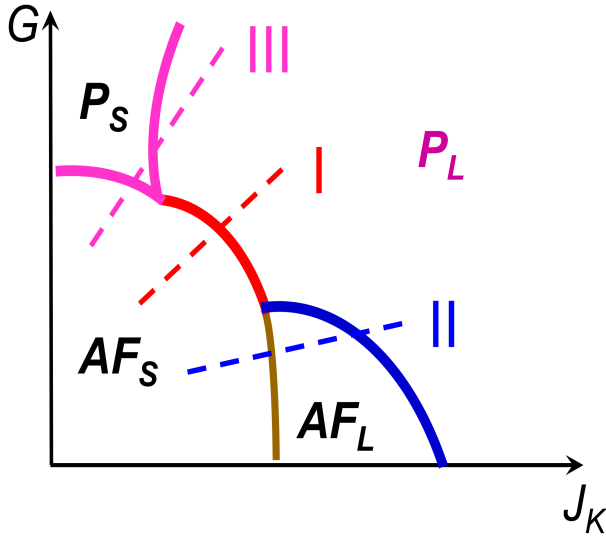


**Figure 2** The  $T = 0$  global phase diagram of the AF Kondo lattice.  $G$  describes magnetic frustration or spatial dimensionality, and  $J_K$  is the normalized Kondo coupling. The four ( $2^2$ ) types of phases,  $AF_S$ ,  $AF_L$ ,  $P_S$ , and  $P_L$  arise since they contain two kinds of distinctions: antiferromagnetism (AF) or paramagnetism (P) on the one hand, and Kondo screening (Fermi surface large, “L”) or Kondo breakdown (Fermi surface small, “S”) on the other hand. The lines “I”, “II”, “III” describe three types of trajectories for the quantum transition.

with heavy quasiparticles and a large Fermi surface [13]. The  $AF_L$  phase corresponds to an AF state in the presence of Kondo screening. It can either be considered as resulting from the  $AF_S$  phase once the Kondo screening sets in, or from the  $P_L$  phase via an SDW instability.

We have discussed the above three phases in some detail before [61,55]. Also alluded to in Ref. [61] is another important feature of this global phase diagram. Along the vertical axis, the conventional Néel order becomes unstable as  $G$  goes beyond some threshold value. The phase at  $G > G_c$  is a paramagnet, restoring the spin-rotational invariance that was broken in the Néel state. It typically still contains valence-bond solid order (spin Peierls), although the cases without any conventional-symmetry-breaking (spin liquid) have also been extensively discussed especially in lattices with strong geometrical frustration.

These considerations lead to the natural possibility of a  $P_S$  phase, a paramagnetic phase with a Kondo breakdown (and, hence, a small Fermi surface) which either breaks or preserves translational invariance. Related Considerations are also being pursued in Refs. [62,63].

This global phase diagram contains three routes for a system to go from the  $AF_S$  phase to the  $P_L$  phase.

- Trajectory “I” is a direct transition between the two. This  $AF_S \rightarrow P_L$  transition gives rise to a local quantum

critical point. A critical Kondo breakdown occurs at the AF QCP, giving rise to a sudden small-to-large jump of the Fermi surface and the vanishing of a Kondo-breakdown scale,  $E_{loc}$  [16, 17].

- Trajectory “II” goes through the  $AF_L$  phase. The quantum critical point at the  $AF_L \rightarrow P_L$  boundary falls in the Hertz-Moriya-Millis type [1, 53, 54].
- Trajectory “III” goes through the  $P_S$  phase. The  $P_S \rightarrow P_L$  transition could describe either a spin liquid to heavy Fermi liquid QCP [18, 19], or a spin Peierls to heavy Fermi liquid QCP.

**5.3 Discussion of the global phase diagram** We now turn to a number of points to elaborate on the global phase diagram.

Consider first the transition along the trajectory “I”. For this transition to be second order, the quasiparticle residues associated with both the small and large Fermi surfaces must vanish as the QCP is approached from either side [16, 17, 39, 61, 64].

The transition along the trajectory “II” involves an intermediate  $AF_L$  phase. This transition can in general be specified [65] through an “order parameter” for the Kondo screening,  $\langle F^y_C \rangle \neq 0$  (where  $F$  is a composite operator involving a spin operator of the local moment and a conduction electron operator), which is non-zero in the  $AF_L$  phase and vanishes in the  $AF_S$ . When the AF order parameter is relatively small, this transition coincides with a Lifshitz transition between Fermi surfaces of different topology [61, 55]. Several authors [66, 67, 68, 69] also identified a Lifshitz transition within a static slave-boson mean-field and related treatments [70, 71] of the Kondo lattice problem. In our global phase diagram, these transitions should be considered as transitions inside the  $AF_L$  region as the AF order parameter is increased [65], and are to be differentiated from the  $AF_L$  to  $AF_S$  transition discussed here.

For a continuous transition between the  $AF_S$  and  $AF_L$  phases, the quasiparticle residues of both the large and small Fermi surfaces must again vanish continuously as the QCP is approached from either side.

The  $P_S$  phase is a state with suppressed Kondo effect. Whether it corresponds to a non-Fermi liquid phase [72] or displays Fermi liquid behavior is an issue that remains to be determined. Two factors come into play. First, what is the nature of the local-moment component? In a two-dimensional square lattice, for instance, spin-1=2 moments at  $G > G_c$  are expected to develop a spin-Peierls order. With geometrical frustration, as occurring in *eg.* a pyrochlore or kagome lattice, it is possible that the local-moment component goes into a spin liquid phase, although this issue is not yet theoretically settled. Second, what is the nature of the Kondo coupling between the local moments and the conduction electrons? The answer will crucially depend on whether the excitation spectrum of the local-moment component is gapped or gapless. If it is gapped, the Kondo coupling will be irrelevant and the low-

energy properties will have a Fermi liquid form. If it is gapless, the behavior of the Kondo coupling can vary depending on its form expressed in terms of the low-energy effective excitations of the local-moment component and the conduction electrons.

**6 Experiments on AF heavy fermions** There are by now many heavy fermion metals in which QCPs have been either explicitly observed, or implicated. We discuss some of them in light of our theoretical considerations.

**6.1 Global phase diagram** A number of heavy fermion materials might be classified according to our global phase diagram, Fig. 2.

In  $\text{CeCu}_{6-x}\text{Au}_x$ , both the pressure- and doping-induced QCPs show the characteristics of local quantum criticality, accessed through trajectory “I”. The field-induced QCP [73], however, has the properties of an SDW QCP. We interpret the field-tuning as taking the trajectory “II”. It will be interesting to explore whether an  $\text{AF}_S\text{-AF}_L$  boundary can be located as a function of magnetic field.

Perhaps the most complete information exists in the pure and doped  $\text{YbRh}_2\text{Si}_2$  system. In the pure  $\text{YbRh}_2\text{Si}_2$ , strong evidence exists that the field-induced transition goes along the trajectory “I” (see below). A surprising recent development came from experiments in the doped  $\text{YbRh}_2\text{Si}_2$ . In the Co-doped  $\text{YbRh}_2\text{Si}_2$ , the field-induced transition seems to travel along trajectory “II” [74]. In the Ir-doped [74] and Ge-doped [62]  $\text{YbRh}_2\text{Si}_2$ , on the other hand, the field-induced transition appears to go along trajectory “III”. Recent experiments in pure  $\text{YbRh}_2\text{Si}_2$  under pressure [75] yield results which are very similar to those of Co-doped  $\text{YbRh}_2\text{Si}_2$  at ambient pressure, suggesting that the results observed in the doped  $\text{YbRh}_2\text{Si}_2$  are in fact intrinsic and do not primarily result from disorder.

$\text{CeIn}_3$  is one of the earliest heavy fermion metals in which an AF QCP was implicated [76]. This system is cubic, and we would expect it to lie in the small  $G$  region of the global phase diagram. Indeed, there is indication that this cubic material displays an  $\text{AF}_S\text{-AF}_L$  Lifshitz transition as a function of magnetic field [77].

It is to be expected that magnetic frustration will help reach the  $P_S$  phase. The heavy fermion system  $\text{YbAgGe}$  has a hexagonal lattice, and, indeed, there is some indication that the  $P_S$  phase exists in this system [78]; lower-temperature measurements over an extended field range, however, will be needed to help establish the detailed phase diagram.

Finally, it is important to note that considerable experiments exist on the nature of the Fermi surface inside the various phases. The  $P_L$  phase was historically established through the observation of the large heavy-fermion Fermi surface [79], while the existence of the  $\text{AF}_S$  phase itself has been supported by the Fermi-surface measurements in a large number of AF heavy fermions [80, 81].

**6.2 Kondo breakdown at the antiferromagnetic QCP** The most direct evidence for the local quantum crit-

ical point occurs in  $\text{YbRh}_2\text{Si}_2$  and in  $\text{CeCu}_{6-x}\text{Au}_x$ . For  $\text{YbRh}_2\text{Si}_2$ , the Fermi-liquid behavior is observed both inside the AF-ordered phase and the field-induced non-magnetic phase [82]. In addition, Hall-coefficient measurements [24, 25] have provided fairly direct evidence for the breakdown of the Kondo effect precisely at the AF QCP. The existence of the Kondo-breakdown scale,  $T_{\text{loc}}$ , has also been seen in both the Hall [24, 25] and thermodynamic [27] experiments.

For  $\text{CeCu}_{6-x}\text{Au}_x$ , the unusual magnetic dynamics [21] observed near the  $x = x_c \approx 0.1$  by early neutron scattering measurements is understood in terms of such a critical Kondo breakdown in the form of local quantum criticality. A divergent effective mass expected in this picture is consistent with the thermodynamic measurement in both the doping and pressure induced QCP in this system [10]. This picture necessarily implies a Fermi-surface jump across the QCP, as well as a Kondo-breakdown energy scale  $E_{\text{loc}}$  going to zero at the QCP, but such characteristics are yet to be probed in  $\text{CeCu}_{6-x}\text{Au}_x$ .

$\text{CeRhIn}_5$  is a member of the Ce-115 heavy fermions [83]. It contains both antiferromagnetism and superconductivity in its pressure-field phase diagram. When a large-enough magnetic-field is applied and superconductivity is removed ( $H > H_{c2}$ ), there is evidence for a single QCP between antiferromagnetic to non-magnetic phases [84, 85]. At this QCP, the de Haas-van Alphen (dHvA) results [26] suggest a jump in the Fermi surface and a divergence in the effective mass.

One of the earliest systems in which anomalous magnetic dynamics was observed is  $\text{UCu}_5\text{-Pd}_x$  [20]. It is tempting to speculate [61] that a Kondo-destroying spin-glass QCP underlies this observation.

**6.3 Spin-density-wave QCP** Neutron scattering experiments have provided some evidence that the AF QCPs in both  $\text{Ce}(\text{Ru}_{1-x}\text{Rh}_x)_2\text{Si}_2$  [22] and  $\text{Ce}_{1-x}\text{La}_x\text{Ru}_2\text{Si}_2$  [23] have the SDW form. Likewise, in  $\text{CeCu}_2\text{Si}_2$ , transport and thermodynamic measurements [86] have indicated that its field-induced QCP belongs to the SDW category.

## 7 Ferromagnetic phases and phase transitions

Compared to their AF counterpart, quantum phase transitions in ferromagnetic heavy fermions have hardly received theoretical attention. While ferromagnetic heavy fermions are rarer to begin with, the list is steadily growing and there are by now more than a dozen such systems being studied experimentally. While the same physics believed to make ferromagnetic quantum transitions first order in the case of weak magnets [87, 88] may also prevail here, it is still important to address whether the Kondo-breakdown physics also appears in the ferromagnetic heavy fermions.

In a recent study [89], we have considered the Kondo lattice model in which the direct exchange between the local moments is ferromagnetic while the Kondo interaction is still antiferromagnetic. It turns out that, due to a separation of energy scales, the ferromagnetic order in the

parameter regime,  $\bar{J}_K \ll \bar{J} \ll W$ , is amenable to an RG analysis. A ferromagnetically ordered phase with a Kondo-breakdown small Fermi surface is seen to be stable, even though the conduction electrons and local moments are strongly coupled to each other. In this  $F_S$  phase, non-Fermi liquid behavior appears over an appreciable range of frequencies and temperatures. These results provide the basis to understand some long-standing puzzles associated with the dHvA observation of a small Fermi surface in some ferromagnetic heavy fermion metals [90]. They may also be related to the non-Fermi liquid behavior observed in the ferromagnetically-ordered state of  $URu_2 \times Re_xSi_2$  [91]. Finally, they raise the prospect for a Kondo-breakdown-type ferromagnetic quantum phase transition.

**8 Summary** We have discussed the physics beyond the order-parameter fluctuations in the quantum criticality of Kondo lattice systems. Of particular interest is the local quantum critical point, which features a critical Kondo breakdown. Microscopic studies on this type of quantum critical point have mostly been based on the extended dynamical mean field theory.

The critical Kondo breakdown at the local quantum critical point leads to a jump in the Fermi surface, a critical suppression of the quasiparticle residues of both the small and large Fermi surfaces, and the vanishing of a Kondo-breakdown scale at the quantum critical point. Considerable experimental evidences for such properties have emerged, which we have summarized.

At the local quantum critical point, there is also a dynamical spin susceptibility which has features of an interacting fixed point. The form, given in Eq. (11), contains a self-energy that has an anomalous frequency dependence, with a fractional exponent, as well as  $\omega = T$  scaling. In contrast to the non-analytic frequency dependence, the momentum dependence of the self-energy is completely regular [which is, in fact, absent in Eq. (11)]. It is interesting to note that recent studies of quantum critical behavior using the gravitational perspective developed in the string-theory context have identified certain symmetry reasons [92] for a single-electron self-energy with non-analytic frequency dependence and smooth momentum dependence [93]. Whether related emergent symmetry can be identified within the gravitational description for the contrasting frequency and momentum dependence in the two-particle self-energy, as appearing in Eq. (11), is an intriguing open question worthy of future studies.

We have also discussed a global phase diagram for the magnetic heavy fermion metals. Detailed theoretical studies to access the overall phase diagram will be much needed.

These developments on the new type of magnetic quantum phase transitions with unusual evolutions of the Fermi surface have not yet been accompanied by corresponding studies on superconductivity. There are many theoretical questions one can ask. Microscopically, whether and how

superconductivity can arise near the Kondo-breakdown local quantum critical point [9,84] is an intriguing open question. Macroscopically, there are general considerations that the entropy accumulation near quantum critical points [94,95] foster the formation of unconventional phases, including unconventional superconductivity [76]. It would be quite meaningful to explore whether a theoretical framework can be developed to implement such considerations.

**Acknowledgements** I am grateful to E. Abrahams, R. Bulla, J. Dai, M. Glossop, P. Goswami, D. Grempel, K. Ingersent, S. Kirchner, E. Pivovarov, J. Pixley, S. Rabello, J. L. Smith, J. Wu, S. Yamamoto, J.-X. Zhu, and L. Zhu for collaborations on the theoretical aspects of this subject. I would also like to thank many colleagues for discussions, particularly P. Coleman and F. Steglich on the global phase diagram. This work has been supported in part by the NSF Grant No. DMR-0706625 and the Robert A. Welch Foundation Grant No. C-1411.

## References

- [1] J. A. Hertz, Phys. Rev. B **14**, 1165–1184 (1976).
- [2] K. G. Wilson and J. Kogut, Phys. Rep. C **12**, 75–200 (1974).
- [3] K. Levin and O. T. Valls, Phys. Rep. **98**, 1–56 (1983).
- [4] P. Pfeuty, Ann. Phys. (N.Y.) **57**, 79 (1970).
- [5] A. P. Young, J. Phys. C **8**, L309 (1975).
- [6] S. Chakravarty, B. I. Halperin, and D. R. Nelson, Phys. Rev. B **39**, 2344–2371 (1989).
- [7] A. V. Chubukov, S. Sachdev, and J. Ye, Phys. Rev. B **49**, 11919–11961 (1994).
- [8] Focus issue: Quantum phase transitions, Nat. Phys. **4**, 167–204 (2008).
- [9] P. Gegenwart, Q. Si, and F. Steglich, Nat. Phys. **4**, 186–197 (2008).
- [10] H. v. Löhneysen, A. Rosch, M. Vojta, and P. Wölfle, Rev. Mod. Phys. **79**, 1015–1075 (2007).
- [11] P. Coleman and A. J. Schofield, Nature **433**, 226–229 (2005).
- [12] G. R. Stewart, Rev. Mod. Phys. **73**, 797–855 (2001).
- [13] A. C. Hewson, The Kondo Problem to Heavy Fermions (Cambridge University Press, Cambridge, 1993).
- [14] S. Doniach, Physica B **91**, 231–234 (1977).
- [15] C. M. Varma, Rev. Mod. Phys. **48**, 219–238 (1976).
- [16] Q. Si, S. Rabello, K. Ingersent, and J. Smith, Nature **413**, 804–808 (2001).
- [17] P. Coleman, C. Pépin, Q. Si, and R. Ramazashvili, J. Phys. Cond. Matt. **13**, R723 (2001).
- [18] T. Senthil, M. Vojta, and S. Sachdev, Phys. Rev. B **69**, 035111 (2004).
- [19] I. Paul, C. Pépin, and M. R. Norman, Phys. Rev. Lett. **98**, 026402 (2007).
- [20] M. C. Aronson, R. Osborn, R. A. Robinson, J. W. Lynn, R. Chau, C. L. Seaman, and M. B. Maple, Phys. Rev. Lett. **75**, 725–728 (1995).
- [21] A. Schröder, G. Aeppli, R. Coldea, M. Adams, O. Stockert, H. v. Löhneysen, E. Bucher, R. Ramazashvili, and P. Coleman, Nature **407**, 351–355 (2000).
- [22] H. Kadowaki, Y. Tabata, M. Sato, N. Aso, S. Raymond, and S. Kawarazaki, Phys. Rev. Lett. **96**, 016401 (2006).

- [23] W. Knafo, S. Raymond, P. Lejay, and J. Flouquet, *Nat. Phys.* **5**, 753–757 (2009).
- [24] S. Paschen, T. Lühmann, S. Wirth, P. Gegenwart, O. Trovarelli, C. Geibel, F. Steglich, P. Coleman, and Q. Si, *Nature* **432**, 881 (2004).
- [25] S. Friedemann, N. Oeschler, S. Wirth, C. Krellner, C. Geibel, F. Steglich, S. Paschen, S. Kirchner, and Q. Si, Fermi-surface collapse and quantum-dynamical scaling near a heavy-fermion quantum critical point, unpublished, 2009.
- [26] H. Shishido, R. Settai, H. Harima, and Y. Ōnuki, *J. Phys. Soc. Jpn.* **74**, 1103–1106 (2005).
- [27] P. Gegenwart, T. Westerkamp, C. Krellner, Y. Tokiwa, S. Paschen, C. Geibel, F. Steglich, E. Abrahams, and Q. Si, *Science* **315**, 1049 (2007).
- [28] T. Senthil, A. Vishwanath, L. Balents, S. Sachdev, and M. P. A. Fisher, *Science* **303**, 1490–1494 (2004).
- [29] A. Auerbach and K. Levin, *Phys. Rev. Lett.* **35**, 3394–3414 (1987).
- [30] A. J. Millis and P. A. Lee, *Phys. Rev. B* (1987).
- [31] M. Oshikawa, *Phys. Rev. Lett.* (2000).
- [32] A. Georges, G. Kotliar, W. Krauth, and M. Rozenberg, *Rev. Mod. Phys.* **68**, 13–125 (1996).
- [33] G. Kotliar and D. Vollhardt, *Phys. Today* **57(3)**, 53–59 (2004).
- [34] M. Jarrell, H. Aklaghpour, and T. Pruschke, *Phys. Rev. Lett.* **70**, 1670–1673 (1993).
- [35] M. J. Rozenberg, *Phys. Rev. B* **52**, 7369–7377 (1995).
- [36] Q. Si and J. L. Smith, *Phys. Rev. Lett.* **77**, 3391–3394 (1996).
- [37] J. L. Smith and Q. Si, *Phys. Rev. B* **61**, 5184–5193 (2000).
- [38] R. Chitra and G. Kotliar, *Phys. Rev. Lett.* **84**, 3678–3681 (2000).
- [39] Q. Si, S. Rabello, K. Ingersent, and J. Smith, *Phys. Rev. B* **68**, 115103 (2003).
- [40] D. Grempel and Q. Si, *Phys. Rev. Lett.* **91**, 026401 (2003).
- [41] J. Zhu, D. Grempel, and Q. Si, *Phys. Rev. Lett.* **91**, 156404 (2003).
- [42] P. Sun and G. Kotliar, *Phys. Rev. Lett.* **91**, 037209 (2003).
- [43] M. Glossop and K. Ingersent, *Phys. Rev. Lett.* **99**, 227203 (2007).
- [44] J. X. Zhu, S. Kirchner, R. Bulla, and Q. Si, *Phys. Rev. Lett.* **99**, 227204 (2007).
- [45] M. Glossop, J. X. Zhu, S. Kirchner, K. Ingersent, Q. Si, and R. Bulla, Kondo destruction in the Kondo lattice model with Ising anisotropy, unpublished, 2009.
- [46] J. Rech, P. Coleman, G. Zarand, and O. Parcollet, *Phys. Rev. Lett.* **96**, 016601 (2006).
- [47] C. Pépin, *Phys. Rev. Lett.* **98**, 206401 (2007).
- [48] L. D. Leo, M. Civelli, and G. Kotliar, *Phys. Rev. Lett.* **101**, 256404 (2008).
- [49] A. H. Nevidomskyy and P. Coleman, *Phys. Rev. Lett.* **102**, 077202 (2009).
- [50] I. Paul and M. Civelli, Signature of Kondo breakdown quantum criticality in optical conductivity, (arXiv:0907.0886) unpublished.
- [51] Q. Si, J. X. Zhu, and D. R. Grempel, *J. Phys.: Condens. Matter* **17**, R1025–R1040 (2005).
- [52] P. Sun and G. Kotliar, *Phys. Rev. B* **71**, 245104 (2005).
- [53] T. Moriya, *Spin Fluctuations in Itinerant Electron Magnetism* (Springer, Berlin, 1985).
- [54] A. J. Millis, *Phys. Rev. B* **48**, 7183–7196 (1993).
- [55] S. J. Yamamoto and Q. Si, *Phys. Rev. Lett.* **99**, 016401 (2007).
- [56] F. D. M. Haldane, *Phys. Rev. Lett.* **50**, 1153–1156 (1983).
- [57] R. Shankar, *Rev. Mod. Phys.* **66**, 129–192 (1994).
- [58] S. Yamamoto and Q. Si, Renormalization group for mixed fermion-boson systems, submitted to *Phys. Rev. B* (arXiv:0906.0014), 2009.
- [59] S. J. Yamamoto and Q. Si, *Physica B* **403**, 1414 (2008).
- [60] T. T. Ong and B. A. Jones, *Phys. Rev. Lett.* **103**, 066405 (2009).
- [61] Q. Si, *Physica B* **378**, 23–27 (2006).
- [62] J. Custers, P. Gegenwart, C. Geibel, F. Steglich, P. Coleman, and S. Paschen, Evidence for non-Fermi liquid phase in Ge-substituted  $\text{YbRh}_2\text{Si}_2$ , unpublished, 2009.
- [63] P. Coleman, this volume (2009).
- [64] T. Senthil, *Ann. Phys. (N.Y.)* **321**, 1669 (2006).
- [65] S. J. Yamamoto and Q. Si, Fermi surface and Kondo breakdown in the antiferromagnetic phases of the Kondo lattice model, unpublished, 2009.
- [66] H. Watanabe and M. Ogata, *Phys. Rev. Lett.* **99**, 136401 (2007).
- [67] L. C. Martin and F. F. Assaad, *Phys. Rev. Lett.* **101**, 066404 (2008).
- [68] M. Vojta, *Phys. Rev. B* **78**, 125109 (2008).
- [69] N. Lanatà, P. Barone, and M. Fabrizio, *Phys. Rev. B* **78**, 155127 (2008).
- [70] C. Lacroix and M. Cyrot, *Phys. Rev. B* **20**, 1969–1976 (1979).
- [71] G. M. Zhang and L. Yu, *Phys. Rev. B* **62**, 76–79 (2000).
- [72] P. W. Anderson, A Fermi sea of heavy electrons (a Kondo lattice) is never a Fermi liquid, arXiv:0810.0279, 2008.
- [73] O. Stockert, M. Enderle, and H. v. Löhneysen, *Phys. Rev. Lett.* **99**, 237203 (2007).
- [74] S. Friedemann, T. Westerkamp, M. Brando, N. Oeschler, S. Wirth, P. Gegenwart, C. Krellner, C. Geibel, and F. Steglich, *Nat. Phys.* **5**, 465–469 (2009).
- [75] Y. Tokiwa, P. Gegenwart, C. Geibel, and F. Steglich, Separation of energy scales in undoped  $\text{YbRh}_2\text{Si}_2$  under hydrostatic pressure, to be published in *JPSJ Letters* and arXiv:0909.1983, 2009.
- [76] N. D. Mathur, F. M. Grosche, S. R. Julian, I. R. Walker, D. M. Freye, R. K. W. Haselwimmer, and G. G. Lonzarich, *Nature* **394**, 39–43 (1998).
- [77] S. E. Sebastian, N. Harrison, C. D. Batista, S. A. T. SA, V. Fanelli, M. Jaime, T. P. Murphy, E. C. Palm, H. Harima, and T. Ebihara, *Proc. Natl. Acad. Sci. USA* **106**, 7741–7744 (2009).
- [78] S. L. Bud'ko, E. Morosan, and P. C. Canfield, *Phys. Rev. B* **71**, 054408 (2005).
- [79] L. Taillefer and G. Lonzarich, *Phys. Rev. Lett.* **60**, 1570–1573 (1988).
- [80] A. McCollam, R. Daou, S. R. Julian, C. Bergemann, J. Flouquet, and D. Aoki, *Physica B* **351**, 1–8 (2005).
- [81] Y. Ōnuki, R. Settai, S. Araki, M. Nakashima, H. Ohkuni, H. Shishido, A. Thamizhavel, Y. Inada, Y. Haga, E. Yamamoto, and T. C. Kobayashi, *Acta Physica Polonica B* **34**, 667–678 (2003).

- [82] J. Custers, P. Gegenwart, H. Wilhelm, K. Neumaier, Y. Tokiwa, O. Trovarelli, C. Geibel, F. Steglich, C. Pépin, and P. Coleman, *Nature* **424**, 524–527 (2003).
- [83] H. Hegger, C. Petrovic, E. G. Moshopoulou, M. F. Hundley, J. L. Sarrao, Z. Fisk, and J. D. Thompson, *Phys. Rev. Lett.* **84**, 4986–4989 (2000).
- [84] T. Park, F. Ronning, H. Q. Yuan, M. B. Salamon, R. Movshovich, J. L. Sarrao, and J. D. Thompson, *Nature* **440**, 65–68 (2006).
- [85] G. Knebel, D. Aoki, J. P. Brison, and J. Flouquet, *J. Phys. Soc. Jpn.* **77**, 114704–114717 (2008).
- [86] P. Gegenwart, C. Langhammer, C. Geibel, R. Helfrich, M. Lang, G. Sparn, F. Steglich, R. Horn, L. Donnevert, A. Link, and W. Assmus, *Phys. Rev. Lett.* **81**, 1501–1504 (1998).
- [87] D. Belitz, T. R. Kirkpatrick, and T. Vojta, *Rev. Mod. Phys.* **77**, 579–632 (2005).
- [88] A. Abanov and A. Chubukov, *Phys. Rev. Lett.* **93**, 255702 (2004).
- [89] S. J. Yamamoto and Q. Si, *Metallic ferromagnetism in the Kondo lattice*, (arXiv:0812.0819) unpublished.
- [90] C. A. King and G. G. Lonzarich, *Physica B* **171**, 161–165 (1991).
- [91] E. D. Bauer, V. S. Zapf, P. C. Ho, N. P. Butch, E. J. Freeman, C. Sirvent, and M. B. Maple, *Phys. Rev. Lett.* **94**, 046401 (2005).
- [92] T. Faulkner, H. Liu, J. McGreevy, and D. Vegh, *Emergent quantum criticality, Fermi surfaces, and AdS2*, arXiv:0907.2694, 2009.
- [93] C. M. Varma, P. B. Littlewood, S. Schmitt-Rink, E. Abrahams, and A. E. Ruckenstein, *Phys. Rev. Lett.* **63**, 1996 – 1999 (1989).
- [94] L. Zhu, M. Garst, A. Rosch, and Q. Si, *Phys. Rev. Lett.* **91**, 066404 (2003).
- [95] A. W. Rost, R. S. Perry, J. F. Mercure, A. P. Mackenzie, and S. A. Grigera, *Science* **325**, 1360 – 1363 (2009).